Earth and Planetary Science Letters 383 (2013) 164–172

Contents lists available at ScienceDirect

Earth and Planetary Science Letters

www.elsevier.com/locate/epsl

Strong lateral variations of lithospheric mantle beneath cratons – Example from the Baltic Shield

H.A. Pedersen [a,b,*], E. Debayle [c], V. Maupin [d], and the POLENET/LAPNET Working Group

[a] Université Grenoble Alpes, ISTerre, F-38041 Grenoble, France
[b] CNRS, ISTerre, F-38041 Grenoble, France
[c] Laboratoire de Sciences de la Terre, Université de Lyon I, CNRS and Ecole Normale Supérieure de Lyon, UMR5570, F-69622 Villeurbanne, France
[d] Department of Geosciences, University of Oslo, Oslo, Norway

ARTICLE INFO

Article history:
Received 21 June 2013
Received in revised form 11 September 2013
Accepted 13 September 2013
Available online 18 October 2013
Editor: P. Shearer

Keywords:
lithosphere
craton
surface waves
Baltic Shield

ABSTRACT

Understanding mechanisms for creation and evolution of Precambrian continental lithosphere requires to go beyond the large-scale seismic imaging in which shields often appear as laterally homogeneous, with a thick and fast lithosphere. We here present new results from a seismic experiment (POLENET-LAPNET) in the northern part of the Baltic Shield where we identify very high seismic velocities ($Vs \sim 4.7$ km/s) in the upper part of the mantle lithosphere and a velocity decrease of ~0.2 km/s at approximately 150 km depth. We interpret this velocity decrease as refertilisation of the lower part of the lithosphere. This result is in contrast to the lithospheric structure immediately south of the study area, where the seismic velocities within the lithosphere are fast down to 250 km depth, as well as to that of southern Norway, where there is no indication of very high velocities in the lithospheric mantle (Vs of ~4.4 km/s). While the relatively low velocities beneath southern Norway can tentatively be attributed to the opening of the Atlantic Ocean, the velocity decrease beneath northern Finland is not easily explained with present knowledge of surface tectonics. Our results show that shield areas may be laterally heterogeneous even over relatively short distances. Such variability may in many cases be related to lithosphere erosion and/or refertilisation at the edge of cratons, which may therefore be particularly interesting targets for seismic imaging.

1. Introduction

The understanding of the structure and evolution of ancient lithosphere has been subject of intense research over the last decade, involving geochemistry, geophysics, rock physics and numerical modeling. It is now well established that the lithosphere in terms of seismic velocities in these areas appear as thick and fast at a large scale (e.g. Gung et al., 2003; Debayle et al., 2005; Legendre et al., 2012) but lack of detail in the seismic models is proving a blocking point for providing well constrained input for numerical models of craton[1] stability and evolution over time. In particular, craton stability is controlled by the vertical and lateral variations in density and viscosity (e.g. Doin et al., 1997; Lenardic and Moresi, 1999; Lenardic et al., 2000; Yoshida, 2012), high viscosity probably being a result of low water contents and the refractory nature of the cratonic mantle lithosphere (Mei and Kohlstedt, 2000; Peslier et al., 2010). In spite of a general longevity of cratons, it is in exceptional cases possible to strongly weaken and possibly erode cratonic lithosphere, as well documented in the eastern part of the North China craton (e.g. Menzies et al., 1993; Lebedev and Nolet, 2003; Zheng et al., 2007; Huang et al., 2009; Xu et al., 2009) and more recently identified in the Saharan Metacraton (Abdelsalam et al., 2011).

In spite of a general similarity between different cratons over a scale of a few hundred to a thousand kilometers (Pedersen et al., 2009), with possibly some systematic difference between Archean domains and Proterozoic mobile belts (Lebedev et al., 2009; Debayle and Ricard, 2012), improvements in the resolution of tomographic models provide increasing evidence of significant lateral variations of seismic structure within cratons at a smaller scale (e.g. James et al., 2001; Poupinet et al., 2003; Bruneton et al., 2004a; Darbyshire et al., 2007, 2013). As we expect that thermal equilibrium is reached in cratons that have not been involved in recent tectonic activity, these variations are likely to be due to lateral variations of composition. Compositional variations within cratons are indeed observed over small scales, even within the same kimberlite pipe, as testified by analysis of mantle xenoliths (e.g. Pearson et al., 2003), but it is still a challenge from a geochemical point of view to observe and quantify systematic vertical and lateral differences of the mantle lithosphere composition at larger scales (few hundreds of kilometers) which would

* Corresponding author.

[1] We use the term craton in its broadest definition, i.e. designating it as an old and stable part of the continental lithosphere, most often composed of an assemblage of Archean and Proterozoic units.

0012-821X/$ – see front matter
http://dx.doi.org/10.1016/j.epsl.2013.09.024

explain the seismic observations. Small differences in abundance of radiogenic elements in the lithospheric mantle could additionally enhance the effect of compositional changes on seismic wave velocities (Hieronymus and Goes, 2010), independently of whether such changes were present from the creation of the cratons, or due to subsequent refertilisation.

Combining seismic and geochemical observations into a comprehensive model of present and past structure of cratonic lithosphere therefore remains a challenge, as the scales of observation do not overlap. The best lateral resolution of seismic models in cratons are obtained by analysis of body waves, but such tomographies usually do not give access to absolute seismic velocities and have very poor depth resolution (e.g. Lévêque and Masson, 1999), limiting their value when we want to compare the results with xenolith data. Tomographic studies using surface waves have better depth resolution and have the advantage of yielding information on absolute shear velocities which are indicative of both temperature and compositional variations. The drawback of surface wave tomography using permanent seismological stations is that the lateral resolution is generally fairly poor. It is however possible to greatly improve the lateral resolution over a limited geographical area by using data from high density temporary seismic networks. Pedersen et al. (2003) and Bodin and Maupin (2008) show that it is possible to achieve a lateral resolution comparable to (at best half of) the investigation depth using such arrays. Due to the presence of seismic noise, dispersion curves with this kind of technique are practically associated with relatively large error bars which make it difficult to use them quantitatively.

In the present study, we follow on this concept while attempting a compromise between the end-members described above: we use dense networks of a few hundred km, which is of comparable size to the largest wavelengths that we study, but all data are combined into the measurement of the average dispersion curve for surface waves propagating across the array. The influence of noise and of heterogeneities outside the array is greatly reduced, and the problem is massively over determined so that the observed dispersion curve is associated with small errors; consequently the subsequent inversion for the shear wave velocity structure with depth is also well constrained. The comparative study between different seismic arrays can then provide well constrained insight into lateral variations in upper mantle structure.

We use this approach for the Baltic Shield where we analyse data from a recent seismic experiment in northern Finland (LAPNET/POLENET, Kozlovskaya et al., 2006) and compare our results with those obtained by a similar approach (Cotte et al., 2001; Bruneton et al., 2004b; Maupin, 2011) in three close locations within the shield: south-central Finland (SVEKALAPKO array, Bock et al., 2001), southern Norway (MAGNUS array, Weidle et al., 2010), and southern Sweden (the somewhat less dense TOR array, Gregersen et al., 1999).

2. Study area

The Baltic Shield, also called Fennoscandian Shield, (Fig. 1) constitutes the northwestern part of the East European Craton. To a first order, it can be separated into two main areas: the Archean to the northeast and the Proterozoic towards the south and west (Gaàl and Gorbatschev, 1987). The Archean comprises the ~3.2–2.5 Ga gneisses and greenstone belts in N–NE Finland and NW Russia, Archean basement covered with Paleoproterozoic sediments, and the Paleoproterozoic Lapland Granulite Belt (~2.5–1.9 Ga). The Proterozoic combines the Svecofennian domain in south-central Finland and western Sweden (~1.95–1.75 Ga) and the later Sveconorwegian domain (~1.1–0.9 Ga) in SW Sweden and most of southern Norway, as well as the Transscandinavian Igneous Belt (~1.85–1.65 Ga). Each of these main areas cover large age

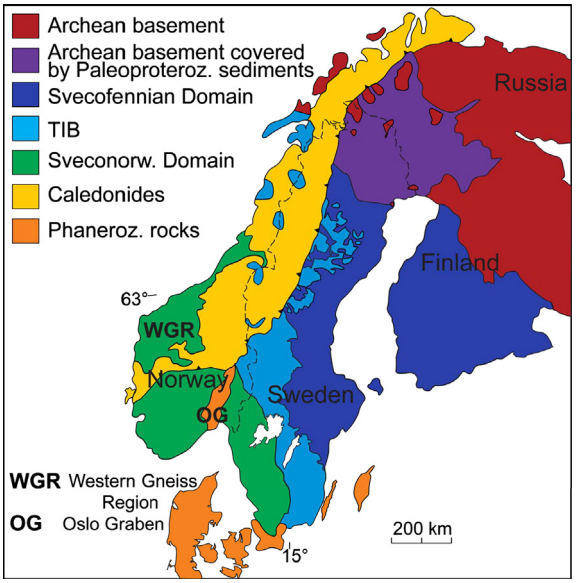

Fig. 1. Simplified tectonic map of the Baltic Shield. The three main domains are: 1. Archean, including Archean basement, Archean basement covered by Paleoproterozoic Sediments and the Paleoproterozoic Lapland Granulite Belt. 2. Proterozoic, composed of the Svecofennian domain, the Sveconorwegian domain and the Transscandinavian Ignous Belt ('TIB'). 3. Caledonides.

variations and tectonic complexities (Gorbatschev and Bogdanova, 1993; Bogdanova et al., 2008).

Except to the east and southeast, the Baltic Shield is bordered by non-cratonic areas: the Barents Sea platform is located north of the Baltic Shield, while we find the West-European Phanerozoic terranes to the south and the continental margin of the North Atlantic Ocean to the west. All these borders have been affected by several collisions and orogenic episodes during geological history. The last episode to the north and northeast is the late Neoproterozoic Timanian orogen (0.66–0.54 Ga; Roberts and Siedlecka, 2002; Pease et al., 2004). To the west and north-west, the Baltic Shield has been affected by the Caledonian orogeny (~0.4 Ga; Roberts, 2003), following the closure of the Tornquist Sea to the south (0.44 Ga; Cocks and Torsvik, 2006).

A large effort has been carried out to collect active seismic data in Finland, the latest during the Finnish Reflection Experiment, FIRE. The FIRE report (Kukkonen and Lahtinen, 2006) provides an excellent review and relevant references of geophysical and geological constraints on the tectonic history in Finland. Of special interest to the LAPNET array is the subdivision of the Archean domain into small tectonic units which have been accreted and deformed during a very complex history including extensional and collisional events, as well as later Paleoproterozoic intrusions (e.g. Daly et al., 2006; Patison et al., 2006; Lahtinen et al., 2008). Fig. 2 shows a more detailed tectonic map of the area covered by the LAPNET array. In spite of the complexities, Poli et al. (2012) showed that the crustal shear velocities only vary by a few percent laterally (mainly associated with slightly elevated velocities within the Lapland Granulite Belt) so lateral variations in crustal structure are not likely to bias the average dispersion curve for the area.

Analysis of data from the temporary seismic broadband SVEKALAPKO experiment in south-central Finland revealed that the relatively unperturbed Svecofennian province in south-central Finland has a simple lithospheric structure with a thick lithospheric root (Sandoval et al., 2004; Bruneton et al., 2004a) which could be explained by approximately uniform composition across the whole thickness of the lithospheric mantle (Bruneton et al., 2004a). On the contrary, the part of the array located on Archean age crust

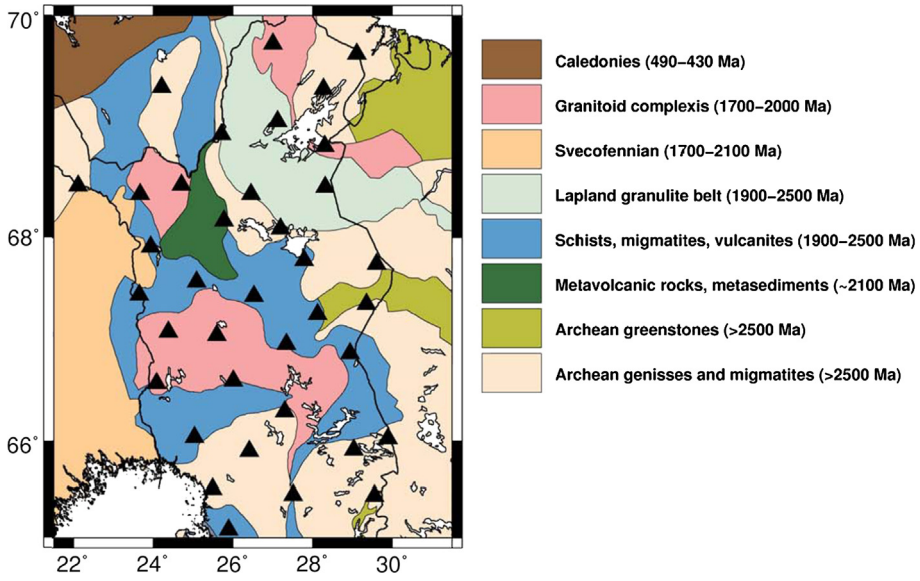

Fig. 2. Tectonic map of the study area. LAPNET seismic stations and permanent stations used in this study are shown as black triangles.

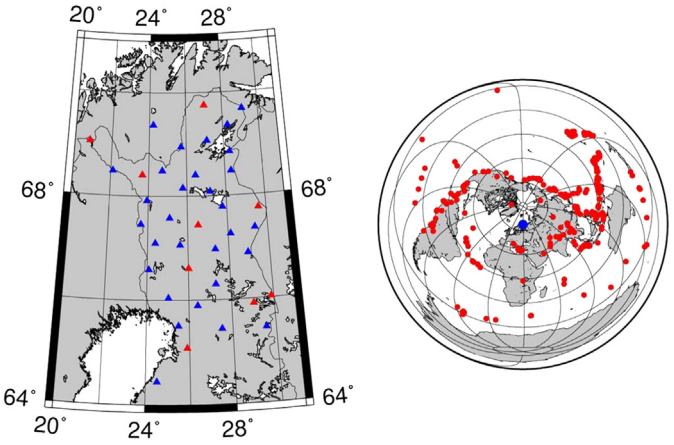

Fig. 3. Data used in this study. Left: seismic broadband station map with temporary LAPNET (blue triangles) and permanent Finnish (red triangles) stations. Right: 288 seismic events (red dots) used for calculating phase velocity dispersion for the LAPNET array. The blue circle indicates the center of the LAPNET array. (For interpretation of the references to color in this figure, the reader is referred to the web version of this article.)

showed a velocity decrease from ~4.73 km/s at 80 km depth to ~4.65 km/s at 120 km depth (Bruneton et al., 2004a), but this observation was poorly constrained due to a small number of stations in that area and a short (6 months) recording period. This observation was a main motivation for the installation of the LAPNET array (see Fig. 3), located immediately north of the SVEKALAPKO array.

3. Lithospheric structure beneath the LAPNET array

To infer the structure of the lithosphere beneath northern Finland, we first calculate a well constrained average dispersion curve of fundamental mode Rayleigh waves, which we subsequently use to infer seismic shear velocity variations with depth.

3.1. Data and data processing

The LAPNET/POLENET temporary seismic array (~275 km × ~460 km) was installed for a two-year period between 2007 and 2009, as part of the International Polar Year. In this study we use vertical component data from LAPNET temporary broadband stations, with the addition of neighboring permanent stations for which continuous datastreams were available (see station configuration in Fig. 3). The complete and continuous dataset for the $2\frac{1}{2}$ years experiment are available at the RESIF data Center (www.resif.fr). The event dataset, available at the same datacenter, comprises all worldwide events for the period with magnitude $\geqslant 6$, on which we applied standard processing (demean and detrend, zero-phase lowpass filter, decimation, deconvolution from instrument response) prior to further processing. Traces with easily identifiable instrumental problems (spikes, poor signal to noise ratio in the 20–50 s period range, faulty components) were automatically removed. Systematically plotting seismic sections lowpassed at 100 s for the events with magnitude $\geqslant 7$ additionally made it possible to identify polarity or instrument response problems, which were corrected in the database, and the data reprocessed.

All preprocessed data were subsequently time-frequency filtered (Levshin et al., 1989) to extract the fundamental mode Rayleigh wave. For each event, we first calculated and visually inspected the group velocity dispersion curve and the raw and filtered data for a centrally located permanent station. We discarded events for which it was not possible to clearly identify and separate the fundamental mode Rayleigh waves, as was the case for some deep events (>50 km), for time windows where waves from different events overlap, or when there was indication of mixing with higher modes. For each accepted event, we subsequently applied the filter, adapted to the epicentral distance, to all stations. This procedure is possible as the interstation distance is much smaller than the epicentral distance and consequently the lateral variations in seismic structure across the array do not influence the filter. For all events we plotted seismic sections in different period intervals, to identify possible remnant problems in data quality. We finally kept 288 events with a good azimuth distribution in spite of predominance of events from the NE quadrant (see Fig. 3).

The mean phase velocity across the array was calculated by analysis of all remaining data. The strategy of analysis is the one of Pedersen et al. (2003) which was further refined to obtain a stable and well constrained dispersion curve. The main steps of the method are discussed here, while we refer to Supplementary material for further detail.

We firstly calculate time delays between all station pairs using the phase of the smoothed interspectra, for a range of frequencies between 10 and 200 s. For each event and frequency, beamforming

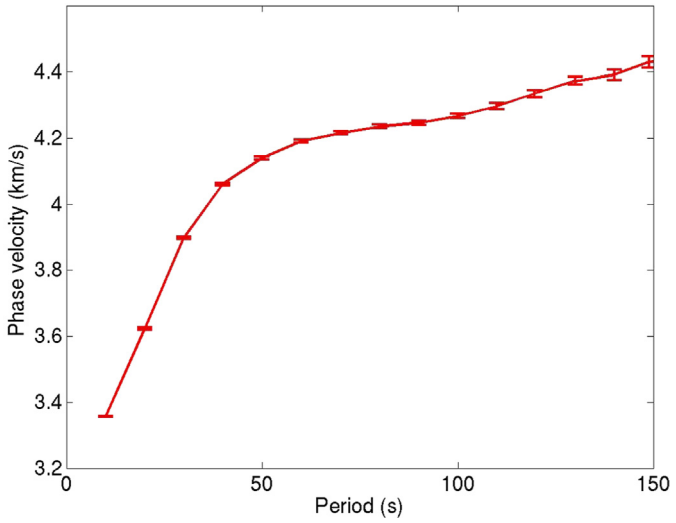

Fig. 4. Observed phase velocity dispersion and associated error bars for fundamental mode Rayleigh waves observed at the LAPNET array.

is carried out to establish the phase velocity, taking into account off great-circle propagation. Finally, the average phase velocity at each frequency is calculated as the simple mean over all events, after further data quality analysis and rejection. The quality analysis (see Supplementary material) showed that our obtained dispersion curve is reliable and associated with small uncertainties between 10 s and 150 s period (see Fig. 4). The error bars shown in Fig. 4 are calculated as the standard deviation of the mean.

3.2. Inversion for shear velocity variations with depth

We subsequently invert the Rayleigh wave dispersion curve for the SV-wave velocity profile below the network. We use a generalized linear inversion (Tarantola and Valette, 1982) in which we control the vertical smoothing of the $Vs(z)$ model via a Gaussian smoothing function of a given width called the correlation length (e.g. Lévêque et al., 1991; Maupin and Cara, 1992) which may vary linearly with depth. In practice the smoothing is integrated through off-diagonal values in the a priori covariance matrix. It is possible to decouple neighboring layers in the model so as to respect velocity jumps, for example at the Moho. The forward calculation of dispersion and partial derivatives takes into account spherical earth geometry, using the software from Saito (1988). Further detail can be found in Maupin (2011). We constrain the allowed velocity variations and iterate the inversion (typically 3 iterations) until the data fit is no longer significantly improved.

There are several well-known limitations in inverting surface wave dispersion curves, in particular when only fundamental mode data are available. This is related to the fact that the dispersion characterizes a very smooth integration over the velocity structure, so the inversion problem is strongly non-unique. All inversions to obtain $Vs(z)$ from (particularly fundamental mode) surface waves are therefore influenced by relatively subjective choices in terms of the parameterization of the model. Non-linear inversions that sample the model space are also very dependent on how the model is set up.

Below we list the four main problems associated with this non-uniqueness, and our strategy for managing them:

- Strongly oscillating models generally give a similar fit to the observed dispersion curve as the one obtained for smoother models. The main difficulty is therefore to allow for the necessary degree of vertical variation in the model to adequately fit the data while not allowing for unresolved variations. Increasing the correlation length with depth is physically logical, as deeper investigation depths are constrained by larger wavelengths. In our case, allowing for an increase in correlation length with depth did not improve the fit to the data so we here focus on results with a constant correlation length. After several trials we choose a constant vertical correlation length of 100 km which allows us to obtain a reliable model. Larger correlation lengths deteriorate the fit to the dispersion curve, while smaller ones introduce non-resolved oscillations.
- There is a trade-off between crustal and uppermost mantle structures. For a 40 km thick crust, this trade-off goes down to approximately 80 km depth (see for example Fig. 18 of Maupin, 2011, or Fig. 4 of Bruneton et al., 2004b). We therefore select our crustal model based on the most recent data available for the area as compiled by Poli et al. (2012) with a 46 km thick crust, and, more importantly, base our conclusions on the $Vs(z)$ model only below 80 km depth. We inverted for the crustal velocity to avoid errors in the shallow structure leaking into the mantle if there is a discrepancy between observed and predicted phase velocities at short periods.
- Errors in the deep structure, well below the resolved part of the model, can migrate into the resolved part of the model. To avoid this problem, we invert for $Vs(z)$ down to depths of 680 km, even though we interpret our results only down to 250 km, i.e. approximately a third of the maximum wavelength in the data.
- The starting model may influence the obtained $Vs(z)$ model. This problem is particularly pronounced if the vertical smoothing is small to moderate. We tested the use of different starting models: due to our conservative choice of vertical correlation length, our conclusions hold for all the starting models we tested. For completeness, we here explain how we constructed the starting model (depicted as a solid black line in Fig. 5). Firstly, we adapted the crustal part of the model using present knowledge from various sources on the local crustal structure, in particular active seismology and receiver function studies. Secondly, below 330 km, we used AK135 (Kennett et al., 1995). The choice of AK135 is not of great importance in our case, as it is close to other global models such as PREM (Dziewonski and Anderson, 1981) below that depth. Between Moho and 220 km depth we use a constant velocity chosen so that the associated dispersion curve approximates the observed one. This approach is partly based on results from Pedersen et al. (2009) which show that constant shear velocities within the lithospheric mantle are adequate to the first order to explain the observed dispersion curves in four shield areas. Finally we impose a constant velocity gradient between

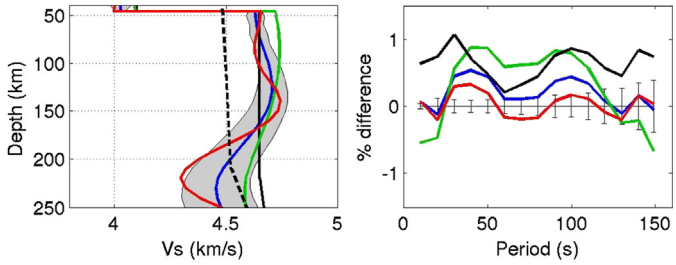

Fig. 5. Left: Earth models from inversion of the dispersion curve of Fig. 4 in the period range 10–150 s. Blue with uncertainties in grey: correlation length 100 km, our preferred solution. Red: Correlation length 50 km. Green: Correlation length 180 km. Black: starting model. Dashed black: AK135. Right: difference (in percent) between the observed dispersion curve (horizontal black line with error bars) and the model with correlation length 100 km (blue), 50 km (red), 180 km (green), starting model (black). (For interpretation of the references to color in this figure, the reader is referred to the web version of this article.)

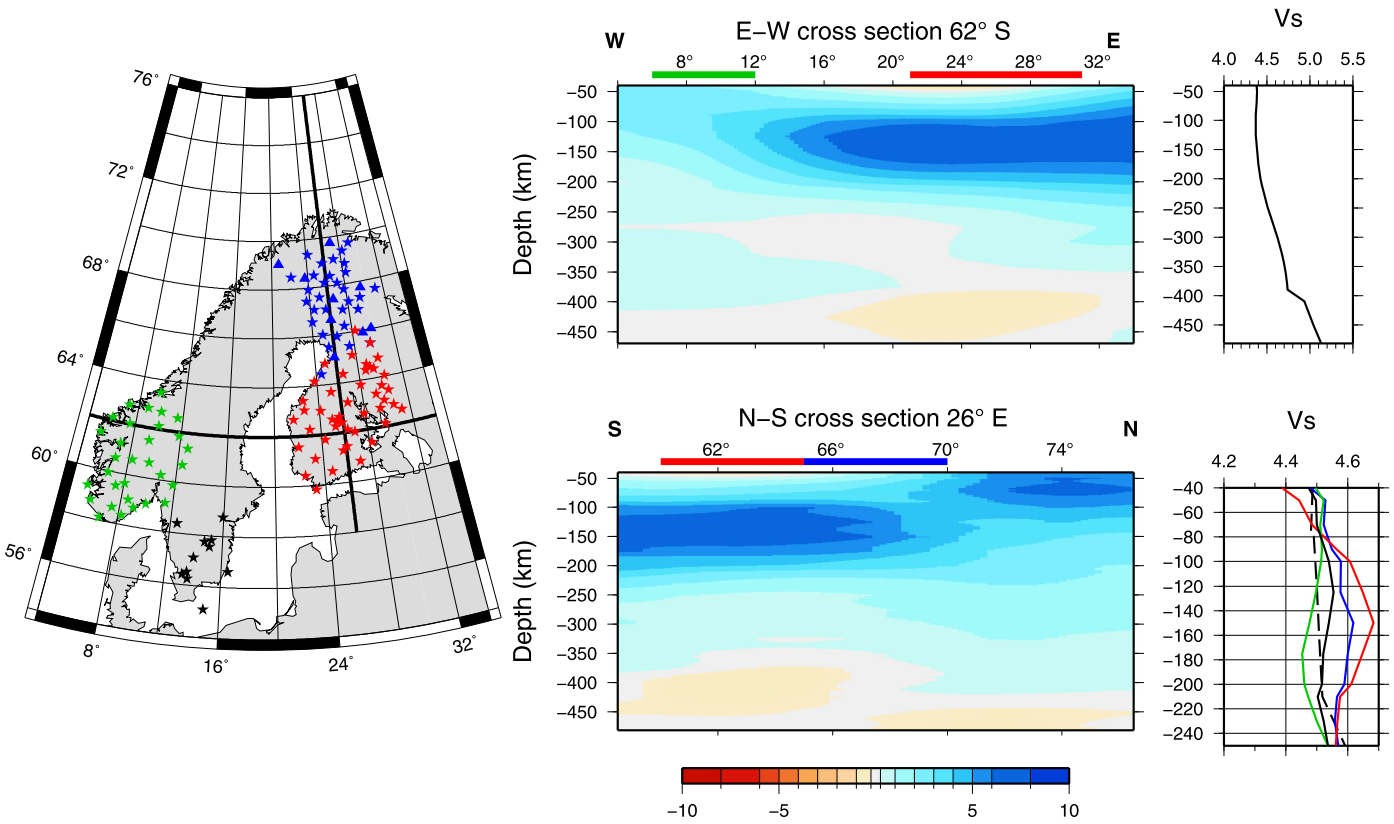

Fig. 6. Left: station map of major seismic broadband experiments in the Baltic Shield. Permanent (blue triangles) and temporary LAPNET (blue stars) stations of the present study; SVEKALAPKO array (red stars); MAGNUS array (green stars); TOR array (black stars). The bold N–S line and E–W curve indicates the location of the cross-sections that are displayed in the middle panel. Middle: cross-sections in DR2012, the global S-wave velocity model of Debayle and Ricard (2012). Top: N–S cross-section along longitude 26°E. Bottom: E–W cross section along latitude 62°N. The approximate positions of the LAPNET, SVEKALAPKO and MAGNUS arrays are indicated with the blue, red and green lines. Right: Top: reference absolute SV velocity profile used to plot the cross sections. Bottom: average SV velocity profiles extracted from DR2102 beneath northern Finland (LAPNET array, blue curve), south-central Finland (SVEKALAPKO array, red curve), southern Sweden (TOR array, black curve) and southern Norway (green curve). The AK135 model is shown by dashed black line.

220 km and 330 km depth to connect the customized lithosphere with AK135.

Fig. 5 presents our preferred model (using 100 km correlation length) and the associated error bars, and the difference in percent from the observed dispersion curve. The figure also shows the result of the inversion using 50 km and 180 km correlation length. The fit using 50 km correlation length is somewhat improved, while a longer correlation length of 180 km significantly deteriorates the fit. The 50 km correlation length leads to unresolved oscillations for the other study areas. So even if the dispersion curve associated with our preferred model does not completely fit within the error bars of the observed dispersion curve, we favor a conservative approach to extract the main parameters that we can compare to other observations in the Baltic Shield.

There are two stable features to highlight here, present in both the 50 km and the 100 km correlation length models. Firstly, the uppermost part of the mantle has significantly higher velocities than the standard earth model AK135, as expected for cratons. The second noticeable feature is that there is a significant and well resolved velocity decrease starting at approximately 150 km depth, which is in contradiction with a deep and depleted lithospheric root. Also, the velocity decrease remains if we exclude the dispersion measurements either at the longest (>130 s) or at the shortest (<50 s) periods. Considering that the average model that we extract covers lateral heterogeneities at even smaller scales, it is possible that the error bars are somewhat underestimated. We therefore verified that the model does not change noticeably if we associate significantly larger error bars (equivalent to the uncertainty at 150 s period) with all the phase velocity measurements. Note that the depth of the velocity decrease is approximately the same for the 50 km and 100 km correlation length models, so we consider that this depth is not defined by the parameterization of the model but rather constrained by the dispersion curve which is slightly depressed in an interval around 100 s period (Fig. 4). This result is in agreement with Legendre et al. (2012) who in a continental scale study show that the northernmost part of the Baltic shields has particularly high velocities (interpreted from the color scale to be approximately 4.65 km/s at 150 km depth) with smaller velocities (of the order of 4.45–4.5 km/s) at 200 km depth. A final feature of our shear-wave profile, but which is poorly resolved due to trade-offs between crust and mantle, is that the models tend towards identical or even lower velocities in the top-most lithosphere (<100 km) as compared to its deeper part. Such observations, which are quite common in shield areas (e.g. Lebedev et al., 2009; Pedersen et al., 2009), are incompatible with constant composition throughout the lithosphere, as demonstrated by Bruneton et al. (2004b).

4. Lateral variability of lithospheric structure in the Baltic Shield

The Baltic Shield is exceptional in that three major seismic broadband experiments have been carried out at three close locations. Fig. 6 places the LAPNET, SVEKALAPKO, and MAGNUS arrays in the context of the global seismic model of Debayle and Ricard (2012). According to this model, the LAPNET experiment (blue) is located at the very edge of a fast area towards the south which can be interpreted as thick cratonic lithosphere (above

which the SVEKALAPKO network (red) was located). The MAGNUS array (green) is located in an area with lower seismic velocities. In the lower right panel, we show the average velocity beneath the four arrays as extracted from the global model. Note that due to use of a simple crustal model in the Debayle and Ricard (2012) model, we can expect crustal errors to leak down to approximately 100 km depth. Care must be taken in comparisons between local and global models, as global models have low lateral resolution, on the order of 1000 km, so the velocity variations are spatially smoothed and locally dampened in amplitude. While the global model shows highest lithospheric velocities beneath the LAPNET and SVEKALAPKO arrays, and lowest velocities for the MAGNUS array, the velocities beneath TOR are clearly reduced due to the neighboring lower velocities beneath Denmark and northern Germany. Also the LAPNET profile, being located on the transition between two large-scale features, show clear signs of the smoothing, while the velocity decrease beneath LAPNET has partially leaked into the SVEKALAPKO profile. So while the global model effectively places the velocities observed locally in a larger context, it is not sufficient to study the detailed lateral variations in absolute velocities.

To compare our results in northern Finland with other parts of the Baltic Shield in a more detailed and consistent way, we re-inverted the phase velocity dispersion curves obtained by other authors for the SVEKALAPKO, MAGNUS and TOR arrays using the same procedure and parameterization as for LAPNET. For SVEKALAPKO, we used the average dispersion curve and crustal model obtained by Bruneton et al. (2004b), while for the MAGNUS array we base the inversion on the phase velocities and crustal model in Maupin (2011). For TOR, we used the dispersion curve by Cotte et al. (2001) and adapted the crustal model from the receiver function study by Alinaghi et al. (2003).

Fig. 7 shows the four velocity profiles obtained. Note that for southern Sweden (TOR array), the observed dispersion curve only covers periods up to 70 s, which is why the model for this area is shown down to 130 km depth only.

The re-inversion of the dispersion curves does not alter the conclusions of the authors of previous studies on the same data, even though the models differ in some details. The qualitative agreement between the cross-sections in the global model and the local models beneath the three arrays is, in spite of the above mentioned issues of smoothing and damping, very good. Highest velocities are found beneath the SVEKALAPKO network down to 250 km depth, lowest velocities beneath the Magnus network, and a mixed situation beneath LAPNET.

As concluded by Maupin (2011), southern Norway is characterized by low upper mantle velocities of approximately 4.4 km/s, in spite of the MAGNUS network being installed on a domain of dominantly Proterozoic age. This velocity is lower than AK135 and close to those of PREM, a sign that a cold and depleted lithosphere is no longer present. In addition to the data presented here, there is evidence for low seismic velocities below southern Norway from other studies, in particular body-wave tomography and regional studies (Maupin et al., 2013; Medhus et al., 2012; Rickers et al., 2013; Wawerzinek et al., 2013; Weidle and Maupin, 2008). This structure is in strong contrast to the three other $Vs(z)$ models which all have high velocities down to approximately 150 km depth. The fundamentally different lithospheric structure beneath southern Norway as compared to the rest of the Baltic Shield is also associated with higher heat flow which translates into higher temperatures in the upper mantle (Artemieva, 2007), a value similar to that of the younger terranes of western Europe to the south. Southern Norway is presently situated at the edge of the Baltic Shield since the opening of the northern mid-Atlantic Ocean (~55 Ma, for a detailed spreading rate history see Mosar et al., 2002). This continent break-up and the passage of

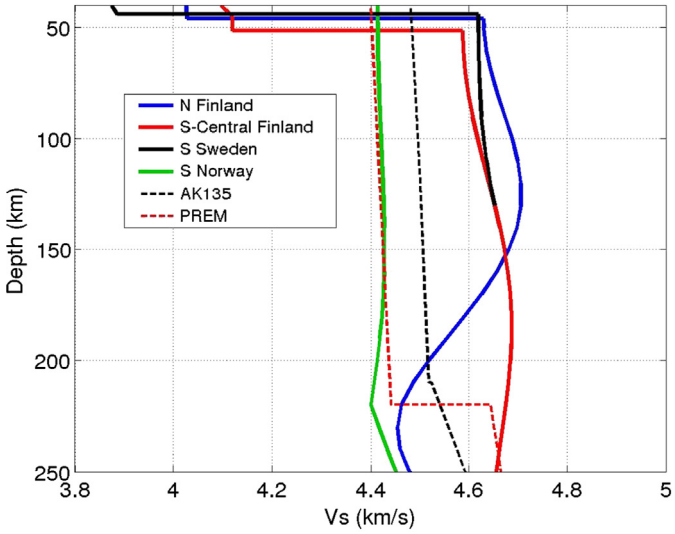

Fig. 7. $Vs(z)$ structure beneath northern Finland (LAPNET array, blue curve), south-central Finland (SVEKALAPKO array, red curve), southern Sweden (TOR array, black curve) and southern Norway (green curve). The southern Sweden model covers depths down to 130 km only due to a limited period range of the observed phase velocity dispersion curve. The standard earth models AK135 and PREM (at a reference period of 1 s) are shown by dashed black and red lines. (For interpretation of the references to color in this figure, the reader is referred to the web version of this article.)

the Iceland hotspot are both good candidates for the refertilisation or thinning of the lithosphere even though the velocities are significantly higher than those found below the North China Craton (Li et al., 2009) where velocities vary from 4.4 km at the Moho to 4.2 km/s at 60 to 100 km depth. The dense ancient lithosphere beneath the North China Craton is thought to have been replaced by younger, less refractory asthenospheric mantle as a result of foundering, stretching or thermal/chemical erosion of the deep lithosphere (e.g. Gao et al., 2008; Menzies et al., 2007; Yang et al., 2008). Whether the same mechanisms can be evoked beneath southern Norway remains speculative at this stage, especially considering the difference in seismic velocities.

SVEKALAPKO, LAPNET and TOR arrays are all located in areas with high velocities in the upper part of the mantle lithosphere, characteristic of cratons (e.g. Pedersen et al., 2009). This observation confirms the presence of depleted cratonic lithosphere beneath the LAPNET array, similar to other cratons and other parts of the Baltic Shield. At greater depth, the velocity decrease identified beneath the LAPNET array in northern Finland is in striking contrast to the average structure beneath the neighboring SVEKALAPKO array in south-central Finland. The latter is characterized by persistent high velocities down to 225–250 km depth, an observation which is also confirmed by P-wave tomography (Sandoval et al., 2004) and by lithospheric thickness as determined by thermobarometry (Kukkonen and Peltonen, 1999). This north-south variation confirms the initial poorly-constrained results from the 3-D seismic structure beneath SVEKALAPKO, where a velocity decrease was tentatively identified, at slightly shallower depths, beneath the northernmost part of the array and adjacent to the LAPNET array.

These observations are in good agreement with the N–S profile in Fig. 6, extracted from the global model of Debayle and Ricard (2012). This profile confirms the observation of a thick cratonic root south of LAPNET while beneath the continental shelf to the north, high velocities are confined to shallower depth. This observation, combined with the extension of shallow high velocities beneath the Barents Sea in the Debayle and Ricard model (2012), is also in good agreement with the model of Levshin et al. (2007) who studied surface wave propagation in the Barents Sea area.

We can at the present stage merely speculate on the origin of the velocity decrease at 150 km depth beneath LAPNET. This area was formed by collision of Archean blocks in the Paleoproterozoic (Bogdanova et al., 2008). The immediate seismic interpretation would be thinning of the Archean lithosphere. In that case, the asthenosphere would be encountered approximately 100 km shallower than beneath the SVEKALAPKO array, in agreement with the difference in thermal lithospheric thickness inferred for these two regions by Artemieva (2007). This interpretation is however not supported by other evidence at hand. Firstly, the surface heat flow does not vary strongly across Finland (Slagstad et al., 2009), with the exception of a small localized area associated with Rapakivi granites. Secondly, a thinner lithosphere above a convecting mantle would induce higher temperatures throughout the lithosphere as compared to the neighboring thicker lithosphere. A temperature increase would lead to reduced seismic velocities within the thinned lithosphere, which is incompatible with the observed very high velocities between the crust and 150 km depth. Our preferred interpretation of the LAPNET model is therefore that the lithospheric thickness, as defined by the intersection of the adiabat with the conductive geotherm, is not significantly different between south-central Finland and northern Finland. The high velocities in the top part of the mantle lithosphere beneath LAPNET could be explained by the presence of refractory, Fe-poor, very dry peridotite. Assuming that the lithosphere is approximately 250 km thick, the lowermost 100 km could have a more fertile composition, richer in iron, clinopyroxene and/or hydrous minerals of which only a small amount is needed to significantly lower the velocities (e.g. Bruneton et al., 2004b). Seismic velocities in a thermally normal cratonic lithosphere can also be reduced below 100–125 km depth by the presence of sulfide melts (Helffrich et al., 2011).

It is unclear when and how changes in composition would have taken place, but due to the presence of continental shelf to the north, oceanic breakup is not a likely candidate. The latest tectonic event that affected the northeast border of the Baltic Shield was the Timanian orogeny (0.66–0.54 Ga; Gee and Pease, 2004; Pease et al., 2004). It is inferred that this orogeny occurred at the end of a subduction that was directed southwestwards, with the Baltic Shield in an overriding position. It is therefore possible that the border of the craton could have been modified at depth during this period. The observed velocity decrease may be too deep to support this explanation as the fluids would have been released at shallower depths during the subduction. Modification of the composition of the deepest part of the lithosphere from localized upwelling of fertile material from the underlying asthenosphere remains another potential explanation. Finally, small-scale erosion at the edge of the cratonic lithosphere through dripping also remains a possibility. Whatever the mechanism was, thermal equilibrium must now be reached to ensure a thermally thick lithosphere, as otherwise the velocities above 150 km depth would be lowered.

Our results confirm and strengthen findings from other areas, where recent high-resolution seismic imaging provide increasing evidence for lateral variations of absolute shear velocities in cratonic lithospheric mantle. At continental scale, Yuan et al. (2011) show lateral heterogeneities within the Superior Province, and notably relatively low velocity beneath the southern part of the Superior Province and the Proterozoic Trans-Hudson Orogen below 150–200 km depth. Several surface wave studies using local seismic networks in Canada also highlight lateral heterogeneity, most spectacularly beneath the Hudson Bay (Darbyshire et al., 2013) where seismic velocities are several percent lower along a NNE–SSW trending area than in the surrounding parts of the Hudson Bay. As in Finland, the velocity variations seem to be higher in the deep lithosphere than in the shallow part. The same is observed in northern Africa (Abdelsalam et al., 2011), where the cratonic areas have similar seismic velocities in the 100–175 km depth range but 5% variation in the 175–250 km depth range, with low velocities beneath the Sahara craton. A recent compilation of several surface wave studies (Kennett et al., 2013) demonstrated that while the Yilgarn in SW Australia has particularly high velocities, lateral variations of shear velocities do not decrease with depth throughout the lithosphere. These authors tentatively interpret part of these variations as changes in lithospheric thickness, but as they point out, and as demonstrated also by the present study (see also Eaton et al., 2009), such interpretations are still very uncertain.

5. Conclusions

The LAPNET data complements results from previous seismic experiments in the Baltic Shield. Together, they provide strong evidence for lateral and vertical heterogeneity within the shield. We observe that there is no clear relationship between the age of the rocks at the surface, and the thickness of the lithosphere. We rather observe that lithospheric structure beneath some areas of the Baltic Shield differs from that of 'normal' cratonic lithosphere. Maybe coincidentally, these areas are located close to the present edge of the shield while furthest away, in Proterozoic south-central Finland, the lithosphere is thick and dominated throughout by high seismic shear velocities. The lithosphere beneath southern Norway is modified throughout, while the new data from northern Finland show modifications below 150 km, which we tentatively interpret as refertilisation of the deepest part of the lithosphere, rather than lithospheric thinning.

Numerical simulations have shown that small-scale erosion is likely to predominantly act at the edge of cratonic lithosphere. Additionally, major tectonic events such as oceanic subduction will take place at the continent edge. Finally, in the case of continental break-up, the effect would be observed at the present shield edges. Our results tend to show that present edges of shields are likely to have some imprint of previous tectonic processes which lead to compositional or temperature change witness and that they may therefore constitute a prime target for investigations aimed at understanding the processes of lithosphere erosion and/or refertilisation, and the mechanisms of craton long-term survival.

Acknowledgements

H. Pedersen received support from the ANR BegDy project, and the Institut Paul Emil Victor. Eric Debayle is supported by the French ANR SEISGLOB No. ANR-11-BLANC-SIMI5-6-016-01. We thank N. Arndt for his insight and comments, and two anonymous reviewers for constructive and fast reviews. Sofie Gradmann from the Geological Survey of Norway kindly provided Fig. 1. Data were obtained through the RESIF data center. The POLENET/LAPNET project is a part of the International Polar Year 2007–2009 and a part of the POLENET consortium, and received financial support from The Academy of Finland (grant No. 122762) and University of Oulu, ILP (International Lithosphere Program) task force VIII, grant No. IAA300120709 of the Grant Agency of the Czech Academy of Sciences, and the Russian Federation: Russian Academy of Sciences (programs Nos. 5 and 9). The Equipment for the temporary deployment was provided by: RESIF – SISMOB (France), EOST-IPG Strasbourg (France), Seismic pool (MOBNET) of the Geophysical Institute of the Czech Academy of Sciences (Czech Republic), Sodankyla Geophysical Observatory (Finland), Institute of Geosphere Dynamics of RAS (Russia), Institute of Geophysics ETH Zürich (Switzerland), Institute of Geodesy and Geophysics, Vienna University of Technology (Austria), University of Leeds (UK). The POLENET/LAPNET working group consists of: Elena Kozlovskaya, Teppo Jämsen, Hanna Silvennoinen, Riitta Hurskainen, Helle Pedersen, Catherine Pequegnat, Ulrich Achauer, Jaroslava Plomerova,

Eduard Kissling, Irina Sanina, Reynir Bodvarsson, Igor Aleshin, Ekaterina Bourova, Evald Brückl, Tuna Eken Robert Guiguet, Helmut Hausmann, Pekka Heikkinen, Gregory Houseman, Petr Jedlicka, Helge Johnsen, Elena Kremenetskaya, Kari Komminaho, Helena Munzarova, Roland Roberts, Bohuslav Ruzek, Hossein Shomali, Johannes Schweitzer, Artem Shaumyan, Ludek Vecsey, Sergei Volosov.

Appendix A. Supplementary material

Supplementary material related to this article can be found online at http://dx.doi.org/10.1016/j.epsl.2013.09.024.

References

Abdelsalam, M.G., Gao, S.S., Liégeois, J.-P., 2011. Upper mantle structure of the Saharan Metacraton. J. Afr. Earth Sci. 60, 328–336.

Artemieva, I., 2007. Dynamic topography of the East European craton: Shedding light upon lithospheric structure, composition and mantle dynamics. Glob. Planet. Change 58, 411–434.

Alinaghi, A., Bock, G., Kind, R., Hanka, W., Wylegalla, K., TOR Group, SVEKALAPKO Group, 2003. Receiver function analysis of the crust and upper mantle from the North German Basin to the Archean Baltic Shield. Geophys. J. Int. 155, 641–652.

Bock, G., SVEKALAPKO Seismic Tomography Working Group, 2001. Seismic probing of Fennoscandian lithosphere. Eos Trans. AGU 82 (621), 628–629.

Bodin, T., Maupin, V., 2008. Resolution potential of surface wave phase velocity measurements at small arrays. Geophys. J. Int. 172, 698–706, http://dx.doi.org/10.1111/j.1365-246X.2007.03668.x.

Bogdanova, S.V., Bingen, B., Gorbatschev, R., Kheraskova, T.N., Kozlov, V.I., Puchkov, V.N., Volozh, Yu.A., 2008. The East European Craton (Baltica) before and during the assembly of Rodinia. Precambrian Res. 160, 23–45.

Bruneton, M., Pedersen, H.A., Farra, V., Arndt, N.T., Vacher, P., SVEKALAPKO Seismic Tomography Working Group, 2004a. Complex lithospheric structure under the central Baltic Shield from surface wave analysis. J. Geophys. Res. 109, B10303.

Bruneton, M., Pedersen, H.A., Vacher, P., Kukkonen, I.T., Arndt, N.T., Funke, S., Friederich, W., Farra, V., SVEKALAPKO Seismic Tomography Working Group, 2004b. Layered lithospheric mantle in the central Baltic Shield from surface waves and xenolith analysis. Earth Planet. Sci. Lett. 226, 41–52.

Cocks, L.R.M., Torsvik, T.H., 2006. European geography in a global context from the Vendian to the end of the Palaeozoic. In: Gee, D.G., Stephenson, R.A. (Eds.), European Lithosphere Dynamics. Mem. Geol. Soc. Lond. 32, 83–95.

Cotte, N., Pedersen, H.A., TOR Working Group, 2001. Sharp transition of the lithospheric structure across the Tornquist Fan as inferred by Rayleigh wave analysis. Tectonophysics 360, 85–88.

Daly, J.S., Balagansky, V.V., Timmerman, M.J., Whitehouse, M.J., 2006. The Lapland–Kola orogen: Paleoproterozoic collision and accretion of the northern Fennoscandian lithosphere. In: Gee, D.G., Stephenson, R.A. (Eds.), European Lithosphere Dynamics. Mem. Geol. Soc. Lond. 32, 579–598.

Darbyshire, F.A., Eaton, D.W., Frederiksen, A.W., Ertolahti, L., 2007. New insights into the lithosphere beneath the Superior Province from Rayleigh wave dispersion and receiver function analysis. Geophys. J. Int. 169, 1043–1068.

Darbyshire, F.A., Eaton, D.W., Bastow, I.D., 2013. Seismic imaging of the lithosphere beneath Hudson Bay: Episodic growth of the Laurentian mantle keel. Earth Planet. Sci. Lett. 373, 170–193.

Debayle, E., Ricard, Y., 2012. A global shear velocity model of the upper mantle from fundamental and higher Rayleigh mode measurements. J. Geophys. Res. 117, B10308, http://dx.doi.org/10.1029/2012JB009288.

Debayle, E., Kennett, B., Priestley, K., 2005. Global azimuthal seismic anisotropy and the unique plate-motion deformation of Australia. Nature 433, 509–512, http://dx.doi.org/10.1038/nature03247.

Doin, M.-P., Fleitout, L., Christensen, U., 1997. Mantle convection and stability of depleted and undepleted continental lithosphere. J. Geophys. Res. 102 (B2), 2771–2787.

Dziewonski, A.M., Anderson, D.L., 1981. Preliminary Reference Earth Model (PREM). Phys. Earth Planet. Inter. 25, 297–356.

Eaton, D., Darbyshire, F., Evans, R., Grütter, R., Jones, A., Yuan, X., 2009. The elusive lithosphere–asthenosphere boundary beneath cratons. Lithos 109, 1–22.

Gaàl, G., Gorbatschev, R., 1987. An outline of the Precambrian evolution of the Baltic Shield. Precambrian Res. 35, 15–52.

Gao, S., Rudnick, R.L., Xu, W.L., Yuan, H.L., Liu, Y.S., Walker, R.J., Puchtel, I.S., Liu, X.M., Huang, H., Wang, X.R., Yang, J., 2008. Recycling deep cratonic lithosphere and generation of intraplate magmatism in the North China craton. Earth Planet. Sci. Lett. 270, 41–53.

Gee, D.G., Pease, V., 2004. The Neoproterozoic Timanide Orogen of eastern Baltica: introduction. Mem. Geol. Soc. Lond. 30, 1–3, http://dx.doi.org/10.1144/GSL.MEM.2004.030.01.01.

Gorbatschev, R., Bogdanova, S., 1993. Frontiers in the Baltic Shield. Precambrian Res. 64, 3–22.

Gung, Y., Panning, M., Romanowicz, B., 2003. Global anisotropy and the thickness of continents. Nature 422 (6933), 707–711.

Gregersen, S., TOR Working Group, 1999. Important findings expected from Europe's largest seismic array. Eos Trans. AGU 80, 1–2.

Helffrich, G., Kendall, J.-M., Hammond, J.O.S., Carroll, M.R., 2011. Sulfide melts and long-term low seismic wavespeeds in lithospheric and asthenospheric mantle. Geophys. Res. Lett. 38, L11301, http://dx.doi.org/10.1029/2011GL047126.

Hieronymus, C.F., Goes, S., 2010. Complex cratonic seismic structure from thermal models of the lithosphere: effects of variations in deep radiogenic heating. Geophys. J. Int. 180, 999–1012.

Huang, Z., Li, H., Zheng, Y., Peng, Y., 2009. The lithosphere of North China Craton from surface wave tomography. Earth Planet. Sci. Lett. 288, 164–173.

James, D.E., Fouch, M.J., VanDecar, J.C., Van der Lee, S., 2001. Tectospheric structure beneath southern Africa. Geophys. Res. Lett. 28, 2485–2488.

Kennett, B.L.N., Engdahl, E.R., Buland, R., 1995. Constraints on seismic velocities in the Earth from traveltimes. Geophys. J. Int. 122, 108–124.

Kennett, B.L.N., Fichtner, A., Fishwick, S., Yoshizawa, K., 2013. Australian Seismological Reference Model (AuSREM): mantle component. Geophys. J. Int. 192, 871–887, http://dx.doi.org/10.1093/gji/ggs065.

Kozlovskaya, E., Poutanen, M., Polenet Working Group, 2006. POLENET/LAPNET—a multi-disciplinary geophysical experiment in northern Fennoscandia during IPY 2007–2008. Geophys. Res. Abstr. 8, 07049.

Kukkonen, I.T., Peltonen, P., 1999. Xenolith controlled geotherm for the central Fennoscandian Shield: implications for lithosphere–asthenosphere relations. Tectonophysics 304, 301–315.

Kukkonen, I.T., Lahtinen, R. (Eds.), 2006. Finnish Reflection Experiment FIRE 2001–2005. Geological Survey of Finland, ISBN 951-690-963-9. Special Paper 43.

Lahtinen, R., Garde, A.A., Melezhik, V.A., 2008. Paleoproterozoic evolution of Fennoscandia and Greenland. Episodes 31 (1), 1–9.

Lebedev, S., Nolet, G., 2003. Upper mantle beneath Southeast Asia from S velocity tomography. J. Geophys. Res. 108 (B1), 2048, http://dx.doi.org/10.1029/2000JB000073.

Lebedev, S., Boonen, J., Trampert, J., 2009. Seismic structure of Precambrian Lithosphere: new constraints from broadband surface-wave dispersion. Lithos 109, 96–111.

Legendre, C.P., Meier, T., Lebedev, S., Friederich, W., Viereck-Götte, L., 2012. A shear wave velocity model of the European upper mantle from automated inversion of seismic shear and surface waveforms. Geophys. J. Int. 191, 282–304.

Lenardic, A., Moresi, L.-N., 1999. Some thoughts on the stability of cratonic lithosphere: effects of buoyancy and viscosity. J. Geophys. Res. 104 (B6), 12747–12758.

Lenardic, A., Moresi, L.-N., Mühlhaus, H., 2000. The role of mobile belts for the longevity of deep cratonic lithosphere: The Crumple Zone Model. Geophys. Res. Lett. 27 (8), 1235–1238.

Lévêque, J.-J., Cara, M., Rouland, D., 1991. Waveform inversion of surface wave data: test of a new tool for systematic investigation of upper mantle structures. Geophys. J. Int. 104, 565–581.

Lévêque, J.J., Masson, F., 1999. From ACH tomographic models to absolute velocity models. Geophys. J. Int. 137, 621–629, http://dx.doi.org/10.1046/j.1365-246x.1999.00808.x.

Levshin, A., Yanovskaya, T., Lander, A., Buckin, B., Barmin, M., Ratnikova, L., Its, E., 1989. In: Keilis-Borok, V.I. (Ed.), Seismic Surface Waves in a Laterally Inhomogeneous Earth. Kluwer, Norwell, M.A.

Levshin, A., Schweitzer, J., Weidle, C., Shapiro, N.M., Ritzwoller, M., 2007. Surface wave tomography of the Barents Sea and surrounding regions. Geophys. J. Int. 170, 441–459.

Li, Y., Wu, Q., Zhang, R., Pan, J., Zhang, F., Zeng, F., 2009. The lithospheric thinning of the North China Craton inferred from Rayleigh waves inversion. Geophys. J. Int. 177 (3), 1334–1342, http://dx.doi.org/10.1111/j.1365-246X.2009.04169.x.

Maupin, V., 2011. Upper-mantle structure in southern Norway from beamforming of Rayleigh wave data presenting multipathing. Geophys. J. Int. 185, 985–1002, http://dx.doi.org/10.1111/j.1365-246X.2012.05449.x.

Maupin, V., Cara, M., 1992. Love-Rayleigh wave incompatibility and possible deep upper mantle anisotropy in the Iberian Peninsula. Pure Appl. Geophys. 138, 429–444.

Maupin, V., Agostini, A., Artemieva, I., Balling, N., Beekman, F., Ebbing, J., England, R.W., Frassetto, A., Gradmann, S., Jocobsen, B.H., Köhler, A., Kvarven, T., Medhus, A.B., Mjelde, R., Ritter, J., Sokoutis, D., Stratford, W., Thybo, H., Wawerzinek, B., Weidle, C., 2013. The deep structure of the Scandes and its relation to tectonic history and present-day topography. Tectonophysics 602, 15–37. http://dx.doi.org/10.1016/j.tecto.2013.03.010.

Medhus, A.B., Balling, N., Jacobsen, B.H., Weidle, C., England, R.W., Kind, R., Thybo, H., Voss, P., 2012. Upper mantle structure beneath the Southern Scandes Mountains and the Northern Tornquist Zone revealed by P-wave travel time tomography. Geophys. J. Int. 189, 1315–1334, http://dx.doi.org/10.1111/j.1365-246X.2012.05449.x.

Mei, S., Kohlstedt, D.L., 2000. Influence of water of plastic deformation od olivine aggregates; 1. diffusion creep regime . J. Geophys. Res. 105, 21471–21481.

Menzies, M.A., Fan, W.-M., Zhang, M., 1993. Paleozoic and Cenozoic lithosphere and the loss of >120 km of Archean lithosphere, Sino-Korean craton, China. In:

Orichard, H., et al. (Eds.), Magmatic Processes and Plate Tectonics. In: Geol. Soc. Spec. Publ., vol. 76, pp. 71–81.
Menzies, M., Xu, Y.G., Zhang, H.F., Fan, W.M., 2007. Integration of geology, geophysics and geochemistry: a key to understanding the North China Craton. Lithos 96, 1–21.
Mosar, J., Lewis, G., Torsvik, T.H., 2002. North Atlantic sea-floor spreading rates: implications for the Tertiary development of inversion structures of the Norwegian–Greenland Sea. J. Geol. Soc. (Lond.) 159, 503–515.
Patison, N.L., Korja, A., Lahtinen, R., Ojala, V.J., FIRE Working Group, 2006. FIRE seismic reflection profiles 4, 4A and 4B: insights into the crustal structure of northern Finland from Ranua to Näätämö. In: Kukkonen, I.T., Lahtinen, R. (Eds.), Finnish Reflection Experiment FIRE 2001–2005. Geological Survey of Finland, ISBN 951-690-963-9. Special Paper 43.
Pearson, D.G., Canil, D., Shirey, S.B., 2003. Mantle samples included in volcanic rocks: xenoliths and diamonds. In: Carlson, Richard W. (Ed.), Holland, Heinrich D., Turekian, Karl K. (Executive Eds.), Treatise on Geochemistry, vol. 2. Elsevier, ISBN 0-08-043751-6, pp. 171–275 (568 pp.).
Pease, V., Dovzhikova, E., Beliakova, L., Gee, D.G., 2004. Late Neoproterozoic granitoid magmatism in the basement to the Pechora Basin, NW Russia: geochemical constraints indicate westward subduction beneath NE Baltica. Mem. Geol. Soc. Lond. 30, 75–85, http://dx.doi.org/10.1144/GSL.MEM.2004.030.01.08.
Pedersen, H.A., Coutant, O., Deschamps, A., Soulage, M., Cotte, N., 2003. Measuring surface wave phase velocities beneath small broadband arrays: test of an improved algorithm and application to the French Alps. Geophys. J. Int. 154, 903–912.
Pedersen, H.A., Fishwick, S., Snyder, D.B., 2009. A comparison of cratonic roots through consistent analysis of seismic surface waves. Lithos 109, 81–95.
Peslier, A.H., Woodland, A.H., Bell, D.R., Lazarov, M., 2010. Olivine water contents in the continental lithosphere and the longevity of cratons. Nature 467, 78–81, http://dx.doi.org/10.1038/nature09317.
Poli, P., Campillo, M., Pedersen, H.A., POLENET/LAPNET Working Group, 2012. Noise directivity and group velocity tomography in a region with small velocity contrasts: the northern Baltic Shield. Geophys. J. Int. 192, 413–424.
Poupinet, G., Arndt, N., Vacher, P., 2003. Seismic tomography beneath stable tectonic regions and the origin and composition of the continental lithospheric mantle. Earth Planet. Sci. Lett. 212, 89–101.
Rickers, F., Fichtner, A., Trampert, J., 2013. The Iceland–Jan Mayen plume system and its impact on mantle dynamics in the North Atlantic region: Evidence form full-waveform inversion. Earth Planet. Sci. Lett. 367, 39–51.
Roberts, D., Siedlecka, A., 2002. Timanian orogenic deformation along the northeastern margin of Baltica, Northwest Russia and Northeast Norway, and Avalonian–Cadomian connections. Tectonophysics 352, 169–184.
Roberts, D., 2003. The Scandinavian Caledonides: event chronology, palaeogeographic settings and likely modern analogues. Tectonophysics 365, 283–299.
Saito, M., 1988. Disper 80: a subroutine package for the calculation of seismic modes solutions. In: Dornboos, D.J. (Ed.), Seismological Algorithms. Academic Press, New York.
Sandoval, S., Kissling, E., Ansorge, J., SVEKALAPKO STWG, 2004. High-resolution body wave tomography beneath the SVEKALAPKO array: II. Anomalous upper mantle structure beneath central Baltic Shield. Geophys. J. Int. 157, 200–214.
Slagstad, T., Balling, N., Elvebakk, H., Midttømme, K., Olesen, O., Olsen, L., Pascal, C., 2009. Heat-flow measurements in Late Palaeoproterozoic to Permian geological provinces in south and central Norway and a new heat-flow map of Fennoscandia and the Norwegian–Greenland Sea. Tectonophysics 473, 341–361, http://dx.doi.org/10.1016/j.tecto.2009.03.007.
Tarantola, A., Valette, B., 1982. Generalized nonlinear inverse problems solved using the least square criterion. Rev. Geophys. 20, 219–232.
Wawerzinek, B., Ritter, J.R.R., Roy, C., 2013. New constraints on the 3-D shear wave velocity structure of the upper mantle underneath Southern Scandinavia revealed from non-linear tomography. Tectonophysics 602, 38–54.
Weidle, C., Maupin, V., 2008. Surface wave tomography for Northern Europe from regional group velocity observations. Geophys. J. Int. 175, 1154–1168, http://dx.doi.org/10.1111/j.1365-246X.2008.03957.x.
Weidle, C., Maupin, V., Ritter, J., Kværna, T., Schweitzer, J., Balling, N., Thybo, H., Faleide, J.I., Wenzel, F., 2010. MAGNUS—A seismological broadband experiment to resolve crustal and upper mantle structure beneath the Southern Scandes Mountains in Norway. Seismol. Res. Lett. 81, 76–84, http://dx.doi.org/10.1785/gssrl.81.1.76.
Xu, X., O'Reilly, S.Y., Griffin, W.L., Zhou, X., 2009. Genesis of young lithospheric mantle in Southeastern China: an LAM–ICPMS trace element study. J. Petrol. 41, 111–148.
Yang, J.H., Wu, F.Y., Widle, S.A., Belousova, E., Griffin, W.L., 2008. Mesozoic decratonization of the North China block. Geology 36, 467–470.
Yoshida, M., 2012. Dynamic role of the rheological contrast between cratonic and oceanic lithospheres in the longevity of cratonic lithosphere: A three-dimensional numerical study. Tectonophysics 532–535, 156–166.
Yuan, H., Romanowicz, B., Fischer, K.M., Abt, D., 2011. 3-D shear wave radially and azimuthally anisotropic velocity model of the North American upper mantle. Geophys. J. Int. 184, 1237–1260.
Zheng, J.P., Griffin, W.L., O'Reilly, S.Y., Yu, C.M., Zhang, H.F., Pearson, N., Zhang, M., 2007. Mechanism and timing of lithospheric modification and replacement beneath the eastern North China Craton: Peridotitic xenoliths from the 100 Ma Fuxin basalts and a regional synthesis. Geochim. Cosmochim. Acta 71, 5203–5225.